1. *Coherent radio Cherenkov radiation detectors*:

Revised February 2013 by S.R. Klein (LBNL/UC Berkeley)

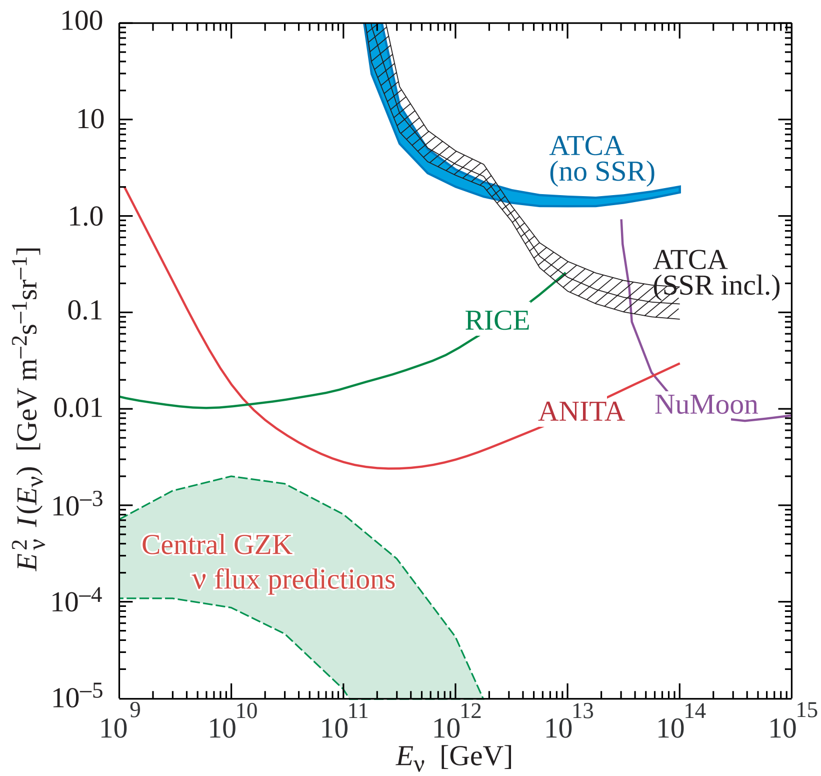

Figure 1: Representative ν flux limits from radio-detection experiments, illustrating the energy ranges for different techniques. Shown are limits from the Rice, ANITA, NuMoon and Lunaska (ATCA) collaborations. NuMoon and Lunaska are low and high frequency lunar scans respectively, showing the strengths of the two different frequency bands. The two limits for ATCA are for different models of the lunar regolith; their separation is a measure of the resultant uncertainty. Also shown, for comparison is the mid-range of flux predictions for GZK neutrinos from Ref. 8.

Radio detectors sensitive to coherent Cherenkov radiation provide an attractive way to search for ultra-high energy cosmic neutrinos. These neutrinos are the only long-range probe of the ultra-high energy cosmos. Protons and heavier nuclei with energies $\gtrsim 5 \times 10^{19}$ eV are limited to ranges of less than 100 Mpc by interactions (photo-excitation) with CMB photons (the GZK effect [1]) , and gamma rays pair-produce from the CMB. When the photoexcited protons/nuclei decay, they produce neutrinos. To detect a useful number of these cosmogenic ("GZK neutrinos") annually (assuming that ultra-high energy cosmic rays are protons) requires a detector of about 100 km^3 in volume. Optical attenuation lengths are less than 200 m in ice or water, so a 100 km^3 detector would require a prohibitive number of sensors.

An alternative is to look for the radio waves from the charged particle showers that are produced when neutrinos interact in a non-conducting medium, as discussed in Sec. 27.

As Gurgen Askaryan pointed out [2], particle showers contains more electrons than positrons, so, for wavelengths larger than their transverse size, emit coherent Cherenkov radiation. The electric field strength is proportional to the neutrino energy; the radiated power goes as its square. Detectors with antennas placed in the active volume have thresholds around 10^{17} eV.

Radiodetection requires a medium with a long absorption length for radio waves. The huge target volumes require that this be a commonly available natural material, usually Antarctic ice or the lunar regolith [5]. Underground salt domes were also considered, but they appear to have too short an attenuation length for radio waves.

The radiation is peaked at the Cherenkov angle (about 56^o in ice). There, the shower produces a short (≈ 1 ns wide) radio pulse. The electric field strength increases linearly with frequency, up to a cut-off wavelength set by the transverse size of the shower and the viewing angle [3,4]. The maximum cut-off is about 1 GHz in ice, and 2.5 GHz in rock/lunar regolith. Away from the Cherenkov angle, the higher frequencies are cut off, and the pulse may be longer. The angular distribution broadens with decreasing frequency, and the frequency spectrum may be used to determine how close a detector is to the Cherenkov cone. This requires a broadband detector; it may also be necessary to account for dispersion and/or refraction as the signal travels from the interaction to the detector. The signal is linearly polarized pointing toward the shower axis. This polarization is a key diagnostic for radiodetection, and can be used to help determine the neutrino direction.

Radio detectors have observed cosmic-ray air showers in the atmosphere. The physics of radio-wave generation in air showers is more complex because there are contributions due to charge separation by charged particles, and from synchrotron radiation from $e^{\pm}$, both due to the Earth's magnetic field. Several experiments have also set limits on radiation due to magnetic monopoles.

1.1. *The Moon as a target:*

Because of its large size and non-conducting regolith, and the availability of large radio-telescopes, the moon is an attractive target [6]. Several representative lunar experiments are listed in Table 1. Conventional radio-telescopes are reasonably well matched to lunar neutrino searches, with natural beam widths not too dissimilar from the size of the Moon. Still, there are some experimental challenges in understanding the signal. The composition of the lunar regolith is not well known, and the attenuation length for radio waves must be estimated. An attenuation length of 9/f(GHz) (m) is often used. The big limitation of lunar experiments is that the 240,000 km target-antenna separation leads to neutrino energy thresholds far above 10^{20} eV.

The frequency range affects the sensitive volume. At low frequencies, radiation is relatively isotropic, so signals can be detected from most of the Moon's surface, for most angles of incidence. At higher frequencies, the electric field is stronger, but radiation is concentrated near the Cherenkov angle, and the geometry limits the sensitivity to interactions near the Moon's limb, where the neutrino also arrives within a fairly narrow angular range. The larger high-frequency attenuation limits the depth below the surface that is probed.

Table 1: Experiments that have set limits on neutrino interactions in the Moon [5]. Some current limits are shown in Fig. 1.

Experiment	Year	Dish Size	Frequency	Bandwidth	Obs. Time
Parkes	1995	64 m	1425 MHz	500 MHz	10 hrs
Glue	1999+	70 m, 34 m	2200 MHz	40-150 MHz	120 hrs
NuMoon	2008	11×25 m	115–180 MHz	—	50 hrs
Lunaska	2008	3× 22 m	1200–1800 MHz	—	6 nights
Resun	2008	4× 25 m	1450 MHz	50 MHz	45 hours

So, higher frequency searches probe lower neutrino energies, but lower frequency searches can set tighter flux limits on high-energy neutrinos. An alternative approach, increasingly viable with modern technology, is to search over a wide frequency range. This introduces a technical challenge in the form of dispersion (frequency dependent time delays) in the ionosphere. The Parkes experiment pioneered the use of de-dispersion filters; this has been taken to a high art by the Lunaska collaboration.

Lunar experiments use several techniques to reject backgrounds, which are mostly anthropogenic. Many experiments use multiple antennas, separated by at least hundreds of meters; by requiring a coincidence within a small time window, anthropogenic noise can be rejected. An alternative approach is to use beam forming with multiple receivers in a single antenna, to ensure that the signal points back to the moon. The limits set by representative lunar experiments are shown in Fig. 1.

In the near future, several large radio detector arrays should reach significantly lower limits. The LOFAR array is beginning to take data with 36 detector clusters spread over Northwest Europe [7]. In the longer term, the Square Kilometer Array (SKA) with 1 km^2 effective area will push thresholds down to near 10^{20} eV.

1.2. *The ANITA balloon experiment:*

To reduce the energy threshold, it is necessary to reduce the antenna-target separation. One such experiment is the ANITA balloon experiment which made two flights around Antarctica, floating at an altitude around 35 km [8]. Its 40 (32 in the first flight) dual-polarization horn antennas scanned the polar ice cap out to the horizon (650 km away). The smaller source-detector separation led to an energy threshold just above 10^{19} eV, slightly above the peak of the GZK neutrino spectrum.

Because of the small angle of incidence, ANITA was able to make use of polarization information; ν signals should be vertically polarized, while most background from cosmic-ray air showers is expected to be horizontally polarized. The analysis treated the multiple antennas as an interferometer; the several-meter separation between antennas led to a pointing accuracy of 0.2-0.4^0 in elevation, and 0.5-1.1^0 in azimuth. The collaboration verified the resolution using radio emitters that they buried in the ice. They then used pointing to eliminate possible anthropogenic backgrounds from inhabited areas of Antarctica.

Antarctic experiments must consider the inhomogeneities in the ice: varying density in the upper ice (the firn) and the variation in radio attenuation length with temperature. ANITA also had to consider the surface roughness, which affects the transition from ice to air. All of these affect the propagation of radio-waves.

The 'firn,' the top 100-200 m of Antarctic ice, marks a transition from packed snow at the surface to solid ice (density 0.92 g/cm^3) below. The density increases gradually with depth. The index of refraction depends on the density, so radio waves bend downward. This curvature reduces the field of view of surface or aerial antennas.

The radio attenuation length depends on the frequency and ice temperature, with attenuation higher in warmer ice. A recent measurement, by the ARA collaboration at the South Pole found an average attenuation length of 670^{+180}_{-66} m [9]. On the Ross Ice Shelf, where the ice is warmer, ARIANNA measures attenuation lengths of 300-500 m, depending on frequency [10].

ANITA has also recently observed radio waves from cosmic-ray air showers; these showers are differentiated from neutrino showers on the basis of the radio polarization and zenith angle distribution [11].

1.3. *Active Volume Detectors:*

The use of radio antennas located in the active volume was pioneered by the RICE experiment, which buried radio antennas in holes drilled for AMANDA [12] at the South Pole. RICE was comprised of 18 half-wave dipole antennas, sensitive from 200 MHz to 1 GHz, buried between 100 and 300 m deep. Each antenna fed an in-situ preamplifier which transmitted the signals to surface digitizing electronics. The array triggered when four or more stations fired discriminators within 1.2 μs, giving it a threshold of about 10^{17} eV.

Two groups are prototyping detectors, with the goal of a detector with an active volume in the 100 km^3 range. Both techniques are modular, so the detector volume scales roughly linearly with the available funding. The Askaryan Radio Array (ARA) is located at the South Pole, while the Antarctic Ross Iceshelf ANtenna Neutrino Array (ARIANNA) is on the Ross Ice Shelf. Both experiments are built of largely independent modules (clusters or stations, respectively), with local triggers based on coincidence between multiple antennas in a module.

One big difference between the two experiments is the depth of their antennas. ARA buries antennas up to 200 m deep in the ice, to avoid the firn, and consequently limited field of view. However, drilling holes raises the costs, and the limited hole diameter (15 cm in ARA) requires compromises between antenna design (particularly for horizontally polarized waves), mechanical support, power and communications. In contrast, ARIANNA places antennas in shallow, near-surface holes. This greatly simplifies deployment and avoid limitations on antenna design, but at a cost of reduced sensitivity to near-surface neutrino interactions.

The current ARA proposal, ARA-37 [9], calls for an array of 37 stations, each consisting of 16 embedded antennas deployed up to 200 m deep below the firn) in several 15-cm diameter boreholes. ARA will detect signals in the frequency range from 150 to

850 MHz for vertical polarization, and 250 MHz to 850 MHz for horizontal polarization. ARA plans to use bicone antennas for vertical polarization, and quad-slotted cylinders for horizontal polarization. The collaboration uses notch filters and surface veto antennas to eliminate most anthropogenic noise, and vetos events when aircraft are in the area, or weather balloons are being launched.

ARIANNA will be located on the Ross Ice Shelf, where $\approx 575\,\text{m}$ of ice sits atop the Ross Sea [10]. The site was chosen because the ice-seawater interface is smooth there, so the interface acts as a mirror for radio waves. The major advantage of this approach is that ARIANNA is sensitive to downward going neutrinos, and should be able to see more of the Cherenkov cone for horizontal neutrinos. One disadvantage of the site is that the ice is warmer, so the radio attenuation length will be shorter. Each ARIANNA station will use 8 log-periodic dipole antennas, pointing downward and arranged in an octagon. The multiple antennas allow for single-station directional and polarization measurements.

References:

1. K. Griesen, Phys. Rev. Lett. **16**, 748 (1966); G.T. Zatsepin and V.A. Kuzmin, JETP Lett. **4**, 78 (1966).
2. G.A. Askaryan, Sov. Phys. JETP **14**, 441 (1962); G.A. Askaryan Sov. Phys. JETP **21**, 658 (1965).
3. D. Saltzberg *et al.*, Phys. Rev. Lett. **86**, 2802 (2001); O. Scholten et al., J. Phys. Conf. Ser. **81**, 012004 (2007).
4. E. Zas, F. Halzen, and T. Stanev, Phys. Rev. **D45**, 362 (1992); J. Alvarez-Muniz, R. A. Vazques, and E. Zas, Phys. Rev. **D62**, 063001 (2000).
5. S.R. Klein, Nucl. Phys. B - Proc. Suppl. **229-232**, 284 (2012)..
6. R.D. Dagkesamanskii and I.M. Zheleznykh, Sov. Phys. JETP Lett. **50**, 233 (1989).
7. S. Buitink *et al.*, `arXiv:1301.5185`.
8. P. Gorham *et al.*, Phys. Rev. **D82**, 022004 (2010); see also the erratum with updated limits, P. Gorham *et al.*, Phys. Rev. **D85**, 049901 (2012).
9. P. Allison *et al.*, Astropart. Phys. **35**, 457 (2012); P. Allison *et al.*, Nucl. Instrum. Methods **A604**, S64 (2009).
10. L. Gerhardt *et al.*, Nucl. Instrum. Methods **A624**, 85-91 (2010); S. Barwick, preprint `arXiv:astro-ph/0610631`; S. Klein, `arXiv:1207.3846`.
11. S. Hoover *et al.*, Phys. Rev. Lett. **105**, 151101 (2010).
12. I. Kravchenko *et al.*, Phys. Rev. **D73**, 082002 (2006); I. Kravchenko *et al.*, Astropart. Phys. **19**, 15 (2003).